Modeling the Heterogeneity of Electrosensory Afferents in Electric Fish

Masterthesis

der Mathematisch-Naturwissenschaftlichen Fakultät
der Eberhard Karls Universität Tübingen

Erstkorrektor: Prof. Dr. Philipp Berens
Zweitkorrektor: Prof. Dr. Jan Benda

Lehrbereich für Neuroethologie

vorgelegt von
Alexander Mathias Ott
Abgabedatum: 21.09.2020

Eigenständigkeitserklärung

Hiermit erkläre ich, dass ich die vorgelegte Arbeit selbstständig verfasst habe und keine anderen als die angegebenen Quellen und Hilfsmittel benutzt habe.

Außerdem erkläre ich, dass die eingereichte Arbeit weder vollständig noch in wesentlichen Teilen Gegenstand eines anderen Prüfungsverfahrens gewesen ist.

_____   _____
Unterschrift   Ort, Datum

Contents

Not to forget: TODO

- update the colors in all plots to be consistent.

- make plot labels consistent (Units: in mV vs [mV])

1 Zusammenfassung

2 Abstract

3 Introduction

1. sensory input important for all life etc.

2. electric fish

   (a) general: habitat,

   (b) as model animal for ethology

   (c) electric organ + eod

   (d) sensory neurons p- and t(?)-type

3. sensory perception

   (a) receptor $\rightarrow$ heterogenic population EXAMPLE!

   (b) further analysis limited by what receptors code for - P-Units encoding

   (c) p-type neurons code AMs

4. goal be able to simulate heterogenic population to analyze full coding properties $\rightarrow$ many cells at the same time needed $\rightarrow$ only possible in vitro/ with model simulations

5. Possible to draw representative values for model parameters to generate a population ?

The environment of an organism holds important information that it needs to survive, react to predators and find food or mates. That means that the ability to sense and process this information is of vital importance for any organism. At the same time the environment also contains a lot of information that is irrelevant to an organism, as such the sensory systems of an organism need to be specialized to extract the information it needs while filtering out the noise and irrelevant information (TODO: ref).

The electric fish *Apteronotus leptorhynchus* (Brown ghost knife fish) generate a sinusoidal electric field with the electric organ in their tail, which they use to find prey, orientation and communication. The different use cases of this electric organ discharge (EOD) come with the necessity to detect small slow amplitude modulations (AMs) in their electric field to detect small prey like insect larvae while also coding for much stronger and faster AMs caused by the EODs of other electric fish in the area. The EOD and changes in it are encoded by electroreceptor organs in the skin. *A. leptorhynchus* have two anatomically different kinds of tuberous electrosensory organs: the T and P type units (TODO: ref, Zakon 1993). Both types encode changes are strongly phase locked to the EOD. The T units (time coder) are more strongly locked to the EOD and fire regularly once every EOD period. They encode the phase of the EOD in their spike timing (TODO: ref). The P units (probability coders) on the other hand do not fire every EOD period instead they fire irregularly with a certain probability that depends on the EOD amplitude (TODO: ref). That way they encode information about the EOD amplitude in their firing probability (TODO: ref). An example of the firing behavior of a P unit is shown in figure 1. An explanation how the different characteristics were computed is below. (TODO: description of the full figure?) P units show strong adaption behavior to changes in EOD amplitude. First they s
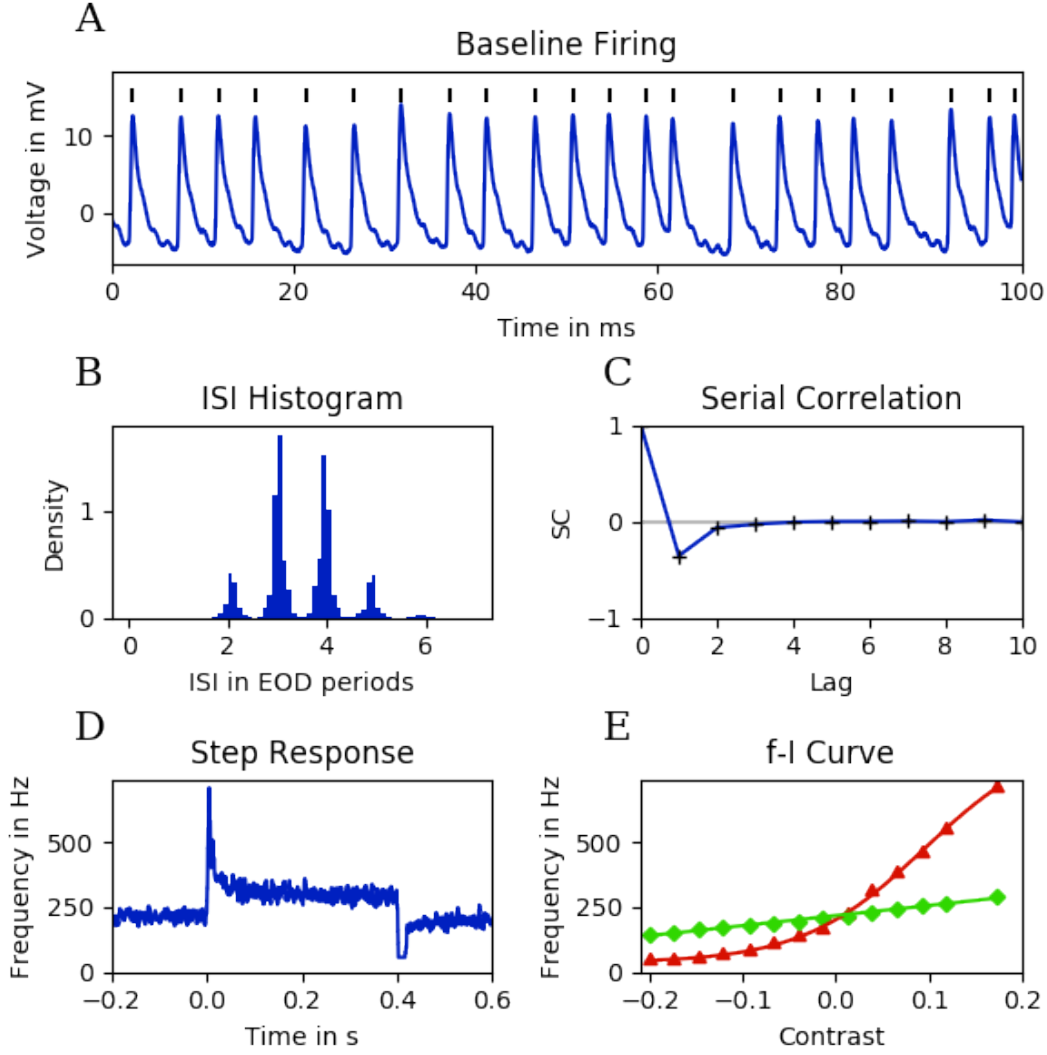
Figure 1: Example behavior of a p-unit with a high baseline firing rate and an EODf of 744 Hz. **A**: A 100 ms voltage trace of the baseline recording with spikes marked by the black lines. **B**: The histogram of the ISI with the x-axis in EOD periods, showing the phase locking of the firing. **C**: The serial correlation of the ISI showing a negative correlation for lags one and two. **D**: The response of the p-unit to a step increase in EOD amplitude. In (TODO: color) the averaged frequency over 10 trials. The p-unit strongly reacts to the onset of the stimulus but very quickly adapts to the new stimulus and then shows a steady state response. **E**: The fi-curve visualizes the onset and steady-state response of the neuron for different step sizes (contrasts). In (TODO: color) the detected onset responses and the fitted Boltzmann, in (TODO: color) the detected steady-state response and the linear fit.

4 Materials and Methods

(TODO: some transition from the introduction)

4.1 Cell recordings

The cell recordings for this master thesis were collected as part of other previous studies (Walz (2013), (Walz et al., 2014))(TODO: ref other studies) and the recording procedure

is described there but will also be repeated below. The recordings of altogether 457 p-units were inspected. Of those 88 fulfilled basic necessary requirements: including a measurement of at least 30 seconds of baseline behavior and containing at least 7 different contrasts with each at least 7 trials for the f-I curve (see below (TODO: ref fi-curve?)). After pre-analysis of those cells an additional 15 cells were excluded because of spike detection difficulties.

The 73 used cells came from 32 *Apteronotus leptorhynchus* (brown ghost knifefish). The fish were between 11–25 cm long (15.8 ± 3.5 cm) and their electric organ discharge (EOD) frequencies ranged between 601 and 928 Hz (753 ± 82 Hz). The sex of the fish was not determined.

The in vivo intracellular recordings of P-unit electroreceptors were done in the lateral line nerve. The fish were anesthetized with MS-222 (100-130 mg/l; PharmaQ; Fording-bridge, UK) and the part of the skin covering the lateral line just behind the skull was removed, while the area was anesthetized with Lidocaine (2%; bela-pharm; Vechta, Germany). The fish were immobilized for the recordings with Tubocurarine (Sigma-Aldrich; Steinheim, Germany, 25–50 μl of 5 mg/ml solution) and placed in the experimental tank (47 × 42 × 12 cm) filled with water from the fish's home tank with a conductivity of about 300μ S/cm and the temperature was around 28°C. All experimental protocols were approved and complied with national and regional laws (files: no. 55.2-1-54-2531-135-09 and Regierungspräsidium Tübingen no. ZP 1/13 and no. ZP 1/16) For the recordings a standard glass mircoelectrode (borosilicate; 1.5 mm outer diameter; GB150F-8P, Science Products, Hofheim, Germany) was used. They were pulled to a resistance of 50–100 MΩ using Model P-97 from Sutter Instrument Co. (Novato, CA, USA) and filled with 1 M KCl solution. The electrodes were controlled using microdrives (Luigs-Neumann; Ratingen, Germany) and the potentials recorded with the bridge mode of the SEC-05 amplifier (npi-electronics GmbH, Tamm, Germany) and lowpass filtered at 10 kHz.

During the recording spikes were detected online using the peak detection algorithm from Todd and Andrews (1999). It uses a dynamically adjusted threshold value above the previously detected trough. To detect spikes through changes in amplitude the threshold was set to 50% of the amplitude of a detected spike while keeping the threshold above a minimum set to be higher than the noise level based on a histogram of all peak amplitudes. Trials with bad spike detection were removed from further analysis. The fish's EOD was recorded using two vertical carbon rods (11 cm long, 8 mm diameter) positioned in front of the head and behind its tail. The signal was amplified 200 to 500 times and band-pass filtered (3 − 1500 Hz passband, DPA2-FX, npi-electronics, Tamm, Germany). The electrodes were placed on iso-potential lines of the stimulus field to reduce the interference of the stimulus in the recording. All signals were digitized using a data acquisition board (PCI-6229; National Instruments, Austin TX, USA) at a sampling rate of 20–100 kHz (54 cells at 20 kHz, 20 at 100 kHz and 1 at 40 kHz)

The recording and stimulation was done using the ephys, efield, and efish plugins of the software RELACS (www.relacs.net). It allowed the online spike and EOD detection, pre-analysis and visualization and ran on a Debian computer.

4.2   Stimulus Protocols

The stimuli used during the recordings were presented from two vertical carbon rods (30 cm long, 8 mm diameter) as stimulus electrodes. They were positioned at either side of the fish parallel to its longitudinal axis. The stimuli were computer generated, attenuated and isolated (Attenuator: ATN-01M, Isolator: ISO-02V, npi-electronics, Tamm, Germany)

and then send to the stimulus electrodes. For this work two types of recordings were made with all cells: baseline recordings and amplitude step recordings for the frequency-Intensity curve (f-I curve). The 'stimulus' for the baseline recording is purely the EOD field the fish produces itself with no external stimulus.

The amplitude step stimulus here is a step in EOD amplitude. The amplitude modulation (AM) is measured as a contrast. The contrast is calculated by dividing the EOD amplitude during the step by the normal EOD amplitude. To be able to cause a given AM in the fish's EOD, the EOD was recorded and multiplied with the modulation (see fig. 2). This modified EOD can then be presented at the right phase with the stimulus electrodes, causing constructive interference and adding the used amplitude modulation to the EOD (Fig. 2). This stimuli construction as seen in equation 1 works for any AM as long as the EOD of the fish is stable.

$$V_{Stim}(t) = EOD(t)(1 + AM(t)) \tag{1}$$

Figure 2: Example of the stimulus construction. At the top a recording of the fish's EOD. In the middle: EOD recording multiplied with the AM, with a step between 0 and 50 ms to a contrast of 30 % (marked in (TODO: color)). At the bottom the resulting stimulus trace when the AM is added to the EOD. (TODO: Umformulieren)
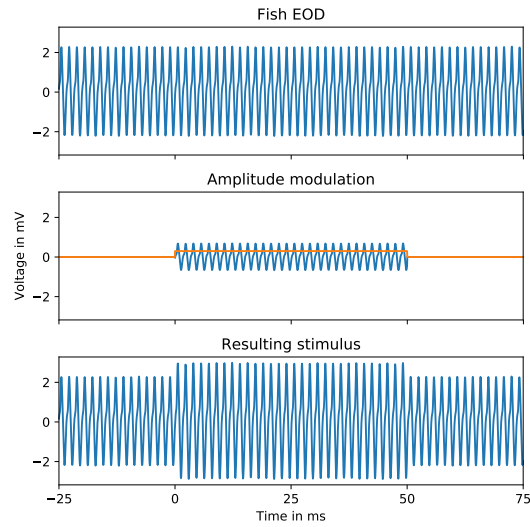
All step stimuli consisted of a delay of 0.2 s followed by a 0.4 s (n=68) or 1 s (n=7) long step and a 0.8 s long recovery time. The contrast range measured was for the most cells 80–120% of EOD amplitude. Some cells were measured in a larger range up to 20–180%. In the range at least 7 contrasts were measured with at least 7 trials, but again many cells were measured with more contrasts and trials. The additionally measured contrasts were used for the model if they had at least 3 trials.

4.3 Cell Characteristics

The cells were characterized by ten parameters: 6 for the baseline and 4 for the f-I curve. For the baseline the mean firing rate was calculated by dividing the number of spikes in the recording by the recording time. Then the set of all interspike intervals (ISI) T was computed and further parameters were calculated from it.

The coefficient of variation

$$CV = \frac{STD(T)}{\langle T \rangle} \tag{2}$$

is defined as the standard deviation (STD) of T divided by the mean ISI, see equation 2 with angled brackets as the averaging operator.

8

The vector strength (VS) is a measure of how strong the cell locks to a phase of the EOD. It was calculated as seen in Eq. 3, by placing each spike on a unit circle depending on the relative spike time t_i of how much time has passed since the start of the current EOD period in relation to the EOD period length. This set of vectors is then averaged and the absolute value of this average vector describes the VS. If the VS is zero the spikes happen equally in all phases of the EOD while if it is one all spikes happen at the exact same phase of the EOD.

$$vs = |\frac{1}{n} \sum_n e^{iwt_i}|$$ (3)

The serial correlation with lag k (SC_k) of T is a measure how the ISI T_i (the i-th ISI) influences the T_{i+k} the ISI with a lag of k intervals. This is calculated as,

$$SC_k = \frac{\langle (T_i - \langle T \rangle)(T_{i+k} - \langle T \rangle) \rangle}{\sqrt{\langle (T_i - \langle T \rangle)^2 \rangle} \sqrt{\langle (T_{i+k} - \langle T \rangle)^2 \rangle}}$$ (4)

with the angled brackets again the averaging operator.

Finally the ISI-histogram was calculated within a range of 0–50 ms and a bin size of 0.1 ms. The burstiness was calculated as the percentage of ISI smaller than 2.5 EOD periods multiplied by the average ISI. This gives a rough measure of how how often a cell fires in the immediately following EOD periods compared to its average firing frequency.
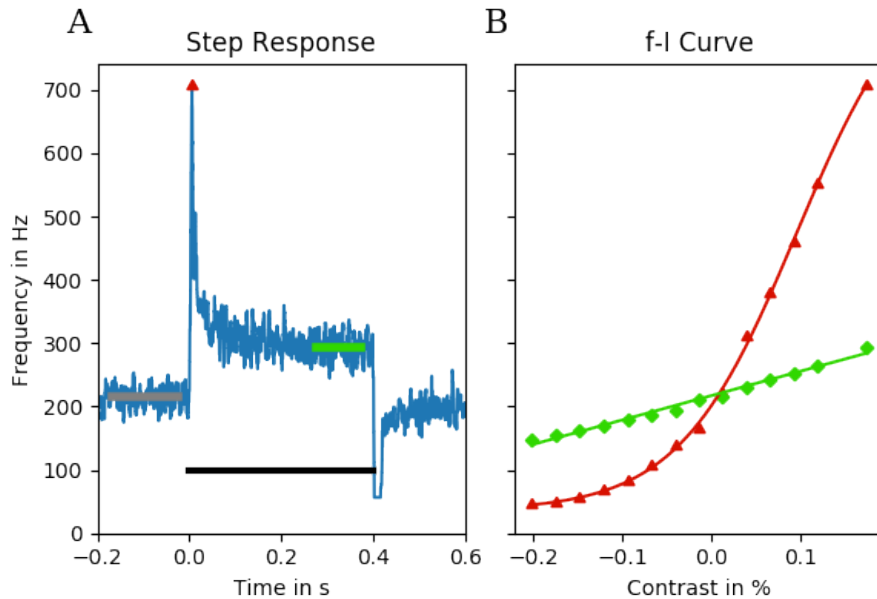

Figure 3: **A**: The averaged response of a cell to a step in EOD amplitude. The step of the stimulus is marked by the back bar. The detected values for the onset (f_0) and steady-state (f_∞) response are marked in (TODO: color). f_0 is detected as the highest deviation from the mean frequency before the stimulus while f_∞ is the average frequency in the 0.1 s time window, 25 ms before the end of the stimulus. **B**: The fi-curve visualizes the onset and steady-state response of the neuron for different stimuli contrasts. In (TODO: color) the detected onset responses and the fitted Boltzmann, in (TODO: color) the detected steady-state response and the linear fit.

As already mentioned in the introduction, p-units react to a step in EOD amplitude with a strong onset response decaying back to a steady state response (fig. 3 A). This adaption behavior of the cell was characterized by the f-I curve measurements. First the ISI frequency trace for each stimulus was calculated. The ISI frequency of a time point t

is defined as $1/T_i$ with T_i the ISI the time point t falls into. This gives a frequency trace starting with the first spike and ending at the last spike. For further analysis all trials of a specific contrast were averaged over the trials with the resolution of the sampling rate. This results in a trial-averaged step response for each contrast as illustrated in figure 3 A. In this firing frequency trace the baseline frequency, the onset f_0 and steady-state f_∞ response were detected. The baseline frequency was measured as the mean of the firing frequency 25 ms after recording start up to 25 ms before the stimulus start. f_0 was then defined as the largest deviation from the baseline frequency, within the first 25 ms after stimulus onset. If there was no deviation farther than the minimum or maximum before the stimulus start, then the average frequency in that 25 ms time window was used. This approximation made the detection of f_0 more stable for small contrasts and trials with high variation. The f_∞ response was estimated as the average firing frequency in the 100 ms time window ending 25 ms before the end of the stimulus (fig. 3 A). Afterwards a Boltzmann:

$$f_0(I) = (f_{max} - f_{min})(1/(1 + e^{-k*(I-I_0)})) + f_{min} \tag{5}$$

was fitted to the onset response and a rectified line:

$$f_\infty(I) = \lfloor mI + c \rfloor_0 \tag{6}$$

(with $\lfloor x \rfloor_0$ the rectify operator) was fitted to the steady-state responses (fig. 3 B).

4.4   Leaky Integrate and Fire Model

The above described cell characteristics need to be reproduced by a simple and efficient model to be able to simulate bigger populations in a reasonable time. The model used in this thesis follows these equations:

$$\tau_m \frac{dV}{dt} = -V + I_{Bias} + \alpha V_{dend} - I_A + \sqrt{2D}\frac{\xi}{\sqrt{\Delta t}} \tag{7}$$

$$\tau_A \frac{dI_A}{dt} = -I_A + \Delta_A \sum \delta(t) \tag{8}$$

$$\tau_{dend} \frac{dV_{dend}}{dt} = -V_{dend} + \lfloor V_{stim} \rfloor_0 \tag{9}$$

Equation 7 describes the leaky dynamics of the membrane voltage with τ_m the membrane time constant, I_{Bias} a bias current, α the cell specific gain factor for V_{dend} the input voltage coming from the dendrite. $\sqrt{2D}$ is the strength of the normal distributed noise ξ. I_A is an adaption current with the dynamics of equation 8. τ_A is the time constant of the adaption, Δ_A its strength and $\delta(t)$ is the spike train of the cell. Equation 9 shows the dynamics of the synapse and dendrite with τ_{dend} the time constant of the dendrite and $\lfloor V_{stim} \rfloor_0$ the rectified stimulus given. Finally the model also includes a refractory period t_{ref}, not shown in above equations, that keeps the membrane voltage V at zero for its duration.

To arrive at this model the simplest commonly used neuron model the perfect integrate-and-fire (PIF) model was stepwise extended. The PIF's voltage can be described in one equation: $\tau_m \frac{dV}{dt} = \frac{I}{R_m}$ with I the stimulus current, R_m the membrane resistance and a voltage threshold V_θ. In this model I is integrated and when this threshold θ is reached the voltage is reset to zero and a spike is recorded (see fig. 4 PIF). The model is useful for basic simulations but cannot reproduce the richer behavior of the p-units, as it has

no memory of previous spikes so it cannot show any adaption behavior and it is also very strongly locked to its limit cycle producing very constant ISI, not allowing the firing flexibility of the p-units.

The next slightly more complex model is the leaky integrate-and-fire (LIF) model:

$$\tau_m \frac{dV}{dt} = -V + IR_m \tag{10}$$

As the name suggests it adds a leakage current to the PIF (fig. 4 LIF). The leakage current adds sub threshold behavior to the model and allows for some more flexibility in suprathresold firing but it is still not flexible enough and cannot reproduce the adaption.

To reproduce the adaption behavior the model needs some form of memory of previous spikes. There are two main ways this can be added to the model as an adaptive current or a dynamic threshold. The biophysical mechanism of the adaption in p-units is unknown because the cell bodies are not accessible for intra-cellular recordings. Following the results of Benda et al. (2010) a negative adaptive current was chosen, because the dynamic threshold causes divisive adaption instead of the subtractive adaption of p-units seen in Benda et al. (2005). This results in an leaky integrate-and-fire model with adaption current (LIFAC) (fig. 4 LIFAC). The added adaptive current follow the dynamics:

$$\tau_A \frac{dI_A}{dt} = -I_A + \Delta_A \sum \delta(t) \tag{11}$$

and gets subtracted from the input current I of of the voltage dynamics eq. 10. It is modeled as an exponential decay with the time constant τ_A and an adaption strength Δ_A. Δ_A is multiplied with the sum of spikes t_i in the spike train ($\delta(t_i)$) of the model cell. For the simulation using the Euler integration this results in an increase of I_A by $\frac{\Delta_A}{\tau_A}$ at every time step where a spike is recorded. (TODO: image of model simulation with voltage adaption and spikes using the toy model?) The input current I from equation 10 is a sum of those two currents and an additional bias current I_{Bias} that is needed to adjusts the cells spontaneous spiking:

$$I = \alpha I_{Input} - I_A + I_{Bias} \tag{12}$$

Note that in this p-unit model all currents are measured in mV because, as mentioned above, the cell body is not accessible for intra-cellular recordings and as such the membrane resistance R_m is unknown (TODO: ref mem res p-units). The input current I_{Input} is the current of the stimulus, an amplitude modulated sine wave mimicking the frequency EOD. This stimulus is then rectified to model the receptor synapse and low-pass filtered with a time constant of τ_{dend} to simulate the low-pass filter properties of the dendrite (fig. 5) according to:

$$\tau_{dend} \frac{dV_{dend}}{dt} = -V_{dend} + \lfloor I_{Input} \rfloor_0 \tag{13}$$

Afterwards it is multiplied with α a cell specific gain factor. This gain factor has the unit of cm because the I_{Input} stimulus represents the EOD with a unit of mV/cm.

Finally, noise and an absolute refractory period were added to the model. The noise ξ is drawn from a Gaussian noise distribution and divided by $\sqrt{\Delta t}$ to get a noise which autocorrelation function is independent of the simulation step size Δt. The implemented form of the absolute refractory period t_{ref} keeps the model voltage at zero for the duration of t_{ref} after a spike. This gives us the full model described in equations 7–9.
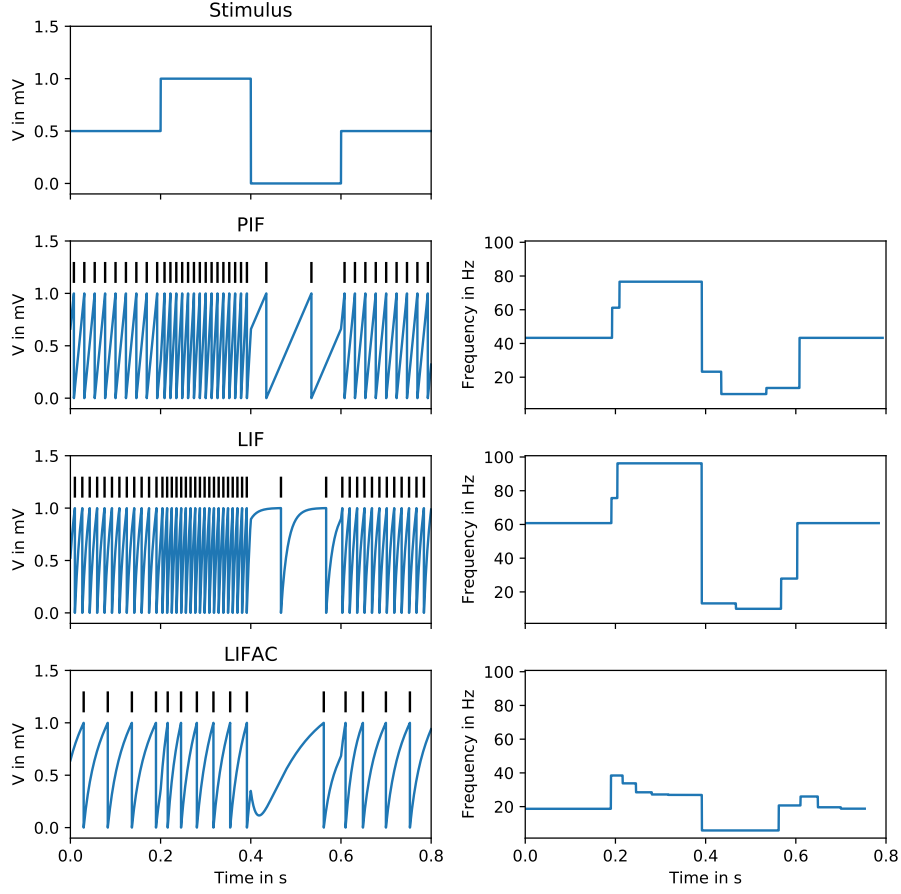
Figure 4: Comparison of different simple models normed to a spontaneous firing rate of 10 Hz stimulated with a step stimulus. In the left column y-axis in mV in the right column the y-axis shows the frequency in Hz. PIF: Shows a continuously increasing membrane voltage with a fixed slope and as such constant frequency for a given stimulus strength. LIF: Approaches a stimulus dependent membrane voltage steady state exponentially Also has constant frequency for a fixed stimulus value. LIFAC: Exponentially approaches its new membrane voltage value but also shows adaption after changes in the stimulus the frequency takes some time to adapt and arrive at the new stable value.

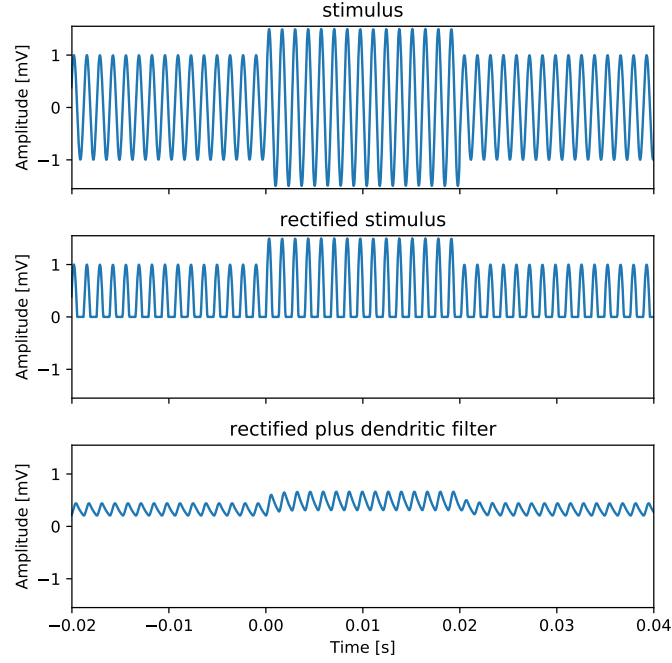Together this results in the dynamics seen in equations 7–9.

Figure 5: The stimulus modification in the model. The fish's EOD is simulated with a sin wave. It is rectified at the synapse and then further low-pass filtered in the dendrite.

parameter	explanation	unit
α	stimulus scaling factor	[cm]
tau_m	membrane time constant	[ms]
I_{Bias}	bias current	[mV]
$\sqrt{2D}$	noise strength	[mV$\sqrt{s}$]
τ_A	adaption time constant	[ms]
Δ_A	adaption strength	[mVms]
τ_{dend}	time constant of dendritic low-pass filter	[ms]
t_{ref}	absolute refractory period	[ms]

Table 1: Overview about all parameters of the model that are fitted.

4.5 Fitting of the Model

The full model has, as described above, eight parameters that need to be fitted so it can reproduce the behavior of the cell. During the fitting and the analysis all models were integrated with at time step of 0.05 ms. The stimuli described in the stimulus protocols section above were recreated for the stimulation of the model during the fitting process. The pure fish EOD was approximated by a simple sine wave of the appropriate frequency, but it was decided to keep the amplitude of the sine wave at one to make the models more comparable. Changes in the amplitude can be compensated for by changing the input scaling factor so there is no qualitative difference.

During the fitting the baseline stimulus was simulated 3 times with 30 s each and the step stimuli were simulated with a delay, step duration and recovery time of each 0.5 s. The contrasts were the same as in the cell recordings. The step stimuli for the different contrasts were each repeated 8 times. The simulated data was analyzed in the same way as the cells (see above).

The error function was constructed from both the baseline characteristics: VS, CV, SC, ISI-histogram and burstiness and the f-I curve: the detections of f_{inf} and f_0 responses for each contrast, the slope of the linear fit into the f_{inf} and the frequency trace of one step response.

The error of the VS, CV, SC, and burstiness was calculated as the scaled absolute difference:

$$err_i = |x_i^M - x_i^C| * c_i \tag{14}$$

with x_i^M the model value for the characteristic i, x_i^C the corresponding cell value and c_i a scaling factor that is the same for all cells but different between characteristics. The scaling factor was used to make all errors a similar size. They are listed in table 2.

The error for the slope of the f_{inf} fit was the scaled relative difference:

$$err_i = |1 - ((x_i^M - x_i^C)/x_i^C)| * c_i \tag{15}$$

For the f_{inf} and f_0 responses the average scaled difference off all contrasts was taken and finally the error for the ISI-histogram and the step-response was calculated with a mean-square error. For the histogram over all bins but for the step response only the first 50 ms after stimulus onset as an error for the adaption time constant.

$$err_i = (\langle (x_i^M - x_i^C)^2 \rangle) * c_i \tag{16}$$

All errors were then summed up for the full error. The fits were done with the Nelder-Mead algorithm of scipy minimize (Gao and Han, 2012). All model variables listed above in table 1 were fit at the same time except for I_{Bias}. I_{Bias} was determined before each fitting iteration and set to a value giving the correct baseline frequency.

behavior	scaling factor
vector strength	100
coefficient of variation	20
serial correlation	10
ISI-histogram	1/600
f_0 detections	0.1
f_∞ detections	1
f_∞ slope	20
f_0 step response	0.001

Table 2: Scaling factors for fitting errors.

5 Results

6 Discussion

References

Benda, J., Longtin, A., and Maler, L. (2005). Spike-frequency adaptation separates transient communication signals from background oscillations. *Journal of Neuroscience*, 25(9):2312–2321.

Benda, J., Maler, L., and Longtin, A. (2010). Linear versus nonlinear signal transmission in neuron models with adaptation currents or dynamic thresholds. *Journal of Neurophysiology*, 104(5):2806–2820.

Gao, F. and Han, L. (2012). Implementing the nelder-mead simplex algorithm with adaptive parameters. *Computational Optimization and Applications*, 51(1):259–277.

Todd, B. S. and Andrews, D. C. (1999). The identification of peaks in physiological signals. *Computers and biomedical research*, 32(4):322–335.

Walz, H. (2013). *Encoding of Communication Signals in Heterogeneous Populations of Electroreceptors*. PhD thesis, Eberhard-Karls-Universität Tübingen.

Walz, H., Grewe, J., and Benda, J. (2014). Static frequency tuning accounts for changes in neural synchrony evoked by transient communication signals. *Journal of Neurophysiology*, 112(4):752–765.